Journal of Cellular Biochemistry 95:1120–1134 (2005)

Inhibition of Extracellular Signal Regulated Kinase (ERK) Leads to Apoptosis Inducing Factor (AIF) Mediated Apoptosis in Epithelial Breast Cancer Cells: The Lack of Effect of ERK in p53 Mediated Copper Induced Apoptosis

Elena A. Ostrakhovitch* and M. George Cherian

Department of Pathology, University of Western Ontario, London, Ontario N6A 5C1, Canada

Abstract Recent studies have shown that MEK/ERK-mediated signals play a major role in regulation of activity of p53 tumor suppressor protein. In this study, we investigated whether or not there is functional interaction between p53 and MEK/ERK pathways in epithelial breast cancer cells exposed to copper or zinc. We demonstrated that expression of wild-type p53 induced by copper or zinc significantly reduced phosphorylation of extracellular signal regulated kinase (ERK) in epithelial breast cancer MCF7 cells. Mutation or suppression of p53 in MDA-MB231 and MCF7-E6 cells, respectively, resulted in a strong ERK phosphorylation in the presence of metals. Weak ERK phosphorylation in MCF7 cells induced by copper or zinc was linked to mitochondrial disruption and apoptosis. Furthermore, inhibition of ERK through addition of PD98059 stimulated p53 activation in MCF7 cells and also led to upregulation of p53 downstream targets, p21 and Bax, which is a proapototic member of Bcl-2 family triggering mitochondrial pore opening. Moreover, blockage of the MEK/ERK pathway caused a breakdown of the mitochondrial membrane potential accompanied by an elevation in the ROS production. Disruption of p53 expression attenuated the depolarization of the mitochondrial membrane and ROS generation. Furthermore, PD98059 initiated apoptosis inducing factor (AIF) translocation from mitochondria to the nucleus in MCF7 cells; which are depleted in caspase 3. Interestingly, repression of MEK/ERK pathway did not intensify the cell stress caused by metal toxicity. Therefore, these findings demonstrate that MEK/ERK pathway plays an important role in downregulation of p53 and cell survival. Inhibition of ERK can lead to apoptosis via nuclear relocation of AIF. However, metal-induced activation of p53 and mitochondrial depolarization appears to be independent of ERK. Our data suggest that copper induces apoptosis through depolarization of mitochondrial membrane with release of AIF, and this process is MEK/ERK independent. J. Cell. Biochem. 95: 1120–1134, 2005.

Key words: ERK; apoptosis; AIF; copper; zinc

Apoptosis is the most important intracellular regulator that eliminates senescent, abnormal, and potentially harmful cells. The deregulation of apoptotic mechanism contributes to a variety of diseases, especially cancer. One of the crucial regulators of cell death is tumor suppressor protein p53. Accumulation of p53 in response to cellular stress can result in growth arrest and apoptosis by upregulation of transcription of a number of specific pro-apoptotic target genes including $p21^{CIP1/Waf1}$, Bax, Noxa, or PUMA [Miyashita and Reed, 1995; Oda et al., 2000; Nakano and Vousden, 2001; Stewart and Pietenpol, 2001; Yu et al., 2001] or suppression of anti-apoptotic genes such as Bcl-2 [Miyashita et al., 1994a,b]. Antiapoptotic members of the bcl-2 family prevent caspase activation and depolarization of mitochondrial membrane, whereas proapoptotic members of this family, such as Bax promote permeability transition pore opening. Under the apoptotic stimuli, Bax translocates to mitochondria directed by p53, where it targets a particular protein on the mitochondrial surface [Marzo et al., 1998; Narita et al., 1998; Shimizu et al., 1999; Schuler et al., 2000; Chipuk et al., 2003, 2004]. As a result, Bax causes permeabilization of the outer mitochondrial membrane (OMM) and the release of apoptogenic factors, including cytochrome-*c* and apoptosis inducing factor (AIF)

*Correspondence to: Dr. Elena A. Ostrakhovitch, Department of Pathology, University of Western Ontario, London, Ontario N6A5C1, Canada. E-mail: eostrakh@uwo.ca

Received 6 December 2004; Accepted 22 February 2005

DOI 10.1002/jcb.20484

[Degli and Dive, 2003]. The AIF once released from mitochondria translocates to the cytosol and to the nucleus where it triggers chromatin condensation and large DNA fragmentation in a caspase-independent manner, which makes AIF particularly important in the cell death in cells, such as MCF7 with depleted caspase 3 or 8 [Susin et al., 1999, 2000; Daugas et al., 2000; Arnoult et al., 2002; Cregan et al., 2002; Fonfria et al., 2002].

The family of mitogen activated protein kinases (MAPK) can be activated in response to variety of stimuli, including free radicals. Oxidative stress induced by metals has been shown to stimulate several members of the MAP kinase [Samet et al., 1998]. The best characterized among MAPKs is extracellular signal regulated kinase (ERK). This kinase is activated by a cascade of phosphorylation that involves initially Ras interaction with Raf-1. Activation of Raf-1, which in turn phosphorylates MEK1 followed by phosphorylation of p44 (ERK1 isoform) and p42 (ERK2 isoform) on tyrosine and threonine residues. Mitogen-activated ERK is known to act as an anti-apoptotic factor by mediating cell proliferation and survival [Xia et al., 1995; Cross et al., 2000]. For example, the inhibition of ERK activity was observed during the apoptosis induced by growth factor withdrawal in PC12 cells [Xia et al., 1995]. Studies carried out in a large number of tumor types have indicated the involvement of MEK/ERK in driving tumor cells proliferation and progression [Sebolt-Leopold and Herrera, 2004]. However, MEK/ERK pathway has been implicated in the cell cycle arrest and the regulation of apoptosis in the absence of survival factor [Sewing et al., 1997; Woods et al., 1997; Makin and Dive, 2001; Pearson et al., 2001]. Therefore, ERK may play a dual role in the regulation of cell survival and death. The way in which ERK mediates these opposing cellular processes can be dependent on regulation of p53 [Wu, 2004]. Activation of MEK/ERK pathway may cause induction of MDM, a major negative regulator of p53, and therefore results in suppression of p53 [Ries et al., 2000; Halaschek-Wiener et al., 2004]. Moreover, it has been shown that MEK inhibitor UO126 downregulated Mdm2 and increased intracellular p53 level [Ries et al., 2000].

A growing body of evidence has indicated that trace elements, such as copper and zinc, play an important role in carcinogenic process [Drake and Sky-Peck, 1989]. It has been shown that the content of copper and zinc in serum and tissue of breast cancer patients was much higher than in benign breast tissues [Cavallo et al., 1991; Koksoy et al., 1997; Jin et al., 1999; Kuo et al., 2002]. An increase in the levels of copper and zinc results in increased oxidative stress in breast cancer cells [Huang et al., 1999]. Moreover, an increase in copper content can result in apoptotic cell death through upregulation of p53 [Narayanan et al., 2001; Ostrakhovitch and Cherian, 2004]. Recent evidence suggests that zinc is involved in the apoptotic cell death as well [Liang et al., 1999; Kondoh et al., 2002]. There are numerous reports concerning zinc-induced mitochondrial apoptogenesis via upregulation of Bax in human cancer cells [Feng et al., 2000, 2002, 2003].

Previous work from our laboratory has shown that copper and zinc cause apoptosis through activation of p53 and resulted expression of downstream targets of p53, such as PIG3 and Bax, responsible for increased generation of the intracellular ROS, as well as disruption of mitochondrial integrity [Ostrakhovitch and Cherian, 2004, 2005]. Moreover, both these metals have been reported to activate MAPK in variety of tumor cells [Hansson, 1996; Samet et al., 1998; Park et al., 2002]. This study was undertaken to elucidate the potential role of MEK/ERK pathway in apoptosis in response to copper and zinc in MCF7 cells with no caspase activity. In addition, we have studied a crosstalk between MEK/ERK and p53 pathways to gain further insight into the mechanisms by which MEK/ERK pathway can regulate apoptosis in human cancer cells.

MATERIALS AND METHODS

Cell Lines

Human breast cancer epithelial cell lines MCF7, estrogen receptor (ER)-positive (ER+) with wild-type p53 (p53+) and MDA-MB-231, ER-negative (ER−) with mutated p53 (p53−), were obtained from ATCC. MCF7-E6 cells are functionally p53-null and derived from epithelial breast cancer MCF7 cells, constitutively expressing the E6 protein from human papilloma virus. MCF7 and MCF7-E6 cells were maintained in DMEM (Dulbecco's modified Eagle's medium, Gibco BRL, Burlington, ON, Canada) supplemented with 10% FBS (fetal bovine serum, Gibco BRL) and antibiotics

(100 units/ml penicillin and 100 mg/ml streptomycin), whereas MDA-MB-231 were grown in RPMI 1640 (Gibco BRL) with 10% FBS. The cells were cultured as monolayers in a humidified incubator, 37°C, 5% CO_2 over a maximum of 30 passages.

Antibodies and Reagents

Anti-Bax was purchased from Oncogene (San Diego, CA); anti-$p21^{Cip/WAF1}$ and anti-p53 (clone FL-393) were purchased from Santa Cruz Biotechnology, Inc. (Santa Cruz, CA), and anti-AIF antibodies was from Chemicon International (Temecula, CA). Anti-GAPDH antibodies were obtained from HyTest Ltd. (Turku, Finland). DCFDA, JC-1, and Acridine Orange were purchased from (Molecular Probes, Eugene,OR). All other reagents were purchased from Sigma Chemical Co (Oakville, ON, Canada). Although in the subsequent discussion we will follow the literature and use the terms "metals" along with "metal ions," it should be always understood that the biological activity of the metals used, such as copper and zinc, is associated with their respective ions.

MTT Assay

The cell viability was measured by MTT assay. About 5×10^3 cells/well (96-well plates) were plated and allowed to grow overnight. These cells were incubated with either DMSO or 30 μM PD98059 for 1 h and treated with 10 and 25 μM of copper or zinc for 4 h. After the test solutions were removed, 50 μl of 0.2 mg/ml MTT (3-(4,5-dimethylthiazol-2-yl)-2,5-diphenyl tetrazolium bromide) solution was added to each well, and the cells were further incubated at 37°C for 4 h. The reaction was stopped by addition of 50 μl 10% SDS/0.01 M HCl to each well. Formazan release from the cells was measured by a microplate reader (Bio-Rad Laboratories Canada Ltd., Mississauga, ON, Canada) at 570 nm. The negative control wells had only culture medium with no cells. Each assay was performed three times in duplicate. The cell viability was calculated as a percent ratio of the absorbance of the samples to appropriate control.

Measurement of Intracellular ROS Generation Using DCFDA

The intracellular ROS generation was measured using 2′,7′-dichlorodihydrofluorescein diacetate (DCFH-DA). Cells were loaded with 20 μM DCFH-DA dissolved in DMSO for 30 min at 37°C. After that cells were washed with PBS, treated with 30 μM PD98059 for 1 h, and then exposed to 10 and 25 μM of $CuSO_4$ or 10 and 25 μM of $ZnSO_4$ in serum-free DMEM for 4 h. Cells were then washed with PBS and fluorescent intensity of 2′,7′-dichlorofluorescein (DCF) was measured by Cary Eclipse fluorescence plate reader (Varian) with excitation at 485 nm and emission at 530 nm. DCFH-DA is a nonfluorescent compound that can readily diffuse across cell membranes and enzymatically hydrolyzed by intracellular esterases to nonfluorescent 2′,7′-dichlorofluorescin (DCFH). This intermediate can be converted to its 2-electron oxidation product, the highly fluorescent compound, DCF with intracellular ROS (hydrogen peroxide, hydroxyl radicals, and others low molecular weight peroxides). To analyze the ability of PD98059 to oxidize DCFH in a cell-free system, DCFH was prepared from DCF-DA by mixing 0.5 ml of 1 mM DCF-DA with 2 ml of 10 mM NaOH at room temperature for 30 min. The mixture was then neutralized to pH 7.4 with 10 ml of 0.25 mM NaH_2PO4 [Myhre et al., 2003].

Determination of the Mitochondrial Membrane Potential ($\Delta\Psi_m$)

5,5′,6,6′-tetrachloro-1,1′, 3,3′-tetraethylbenzamidazolo-carbocyanin iodide (JC-1) is a membrane potential-sensitive dye that accumulates in mitochondria and subsequently forms J-aggregates from monomers, which fluorescence at 590 nm, and has been suggested to reflect the membrane potential of the mitochondria. Cells were incubated with 30 μM PD98059 for 1 h and then treated with copper (10 and 25 μM) or zinc (10 and 25 μM) for 4 h, and the mitochondrial membrane potential was analyzed in the cells by staining them with 10 μM of JC-1 for 10 min. The intensity of fluorescence was immediately measured at 527 and 590 nm emission wavelength (with excitation at 488 nm), corresponding to the fluorescence peak of the monomer and that of the aggregate, respectively. JC staining shifts from red to green when the mitochondrial potential drops to more depolarized values. Proportion of cells with depolarized mitochondria was calculated as a ratio of the intensities at 590 nm (red) and 527 nm (green). Relative change in proportion of cells with depolarized mitochondria was calculated as the ratio of red/green fluorescence intensity for metal treated to

control (untreated) samples. The decrease in the red/green fluorescence intensity ratio indicates mitochondrial depolarization and loss of mitochondrial membrane potential ($\Delta\Psi_m$).

Quantification of Apoptosis

Apoptotic cells were visualized by incubation with Hoechst 33342. Human epithelial breast cancer MCF7 cells were seeded into 6-well plate containing glass cover slips, and allowed to grow into confluent monolayers. Cells were incubated for 1 h with either DMSO or 30 μM PD98059, and then exposed to various concentrations of copper and zinc for additional 4 h. After treatment, cells were washed with PBS and 0.5 ml of 1 μg/ml Hoechst 33342 in PBS was added. The cells were examined by fluorescence microscopy (Zeiss Axiovert 100 TV fluorescence microscope (Carl Zeiss, Germany). Then, apoptosis was expressed as a percent of fragmented Hoechst positive nuclei versus total Hoechst-positive nuclei. Apoptotic cells were identified by typical apoptotic features such as chromatin condensation, nuclear fragmentation, and shrinking.

Protein Extraction and Western Blot Analysis

After the treatment, cells were washed once with cold PBS, scraped off on ice using 100 μl of lysate buffer per a 3 cm^2 dish, and kept on ice. The lysate buffer consisted of 20 mM Tris (pH 7.5), 150 mM NaCl, 1% (w/v) Triton X-100, phosphatase inhibitors (100 mM Na_3VO_4, 10 mM NaF), and protease inhibitors (1 mM PMSF, 10 μg/ml aprotinin). The whole cell lysates were vortexed and centrifuged at 12,000*g* for 20 min at 4°C. The resulting supernatants were transferred to fresh Eppendorf tubes, and the protein concentration was determined using a detergent-compatible Bio-Rad protein assay (Bio-Rad Laboratories Canada Ltd.). All cell lysates were normalized for protein and were combined with SDS-Laemmli sample buffer. Aliquotes of the supernatant were frozen and stored at −70°C.

Sixty micrograms of each cell lysate was separated by 10% SDS–PAGE and transferred to polyvinylidene dufluoride (PVDF) membrane membranes (Bio-Rad Laboratories Canada Ltd.), blocked with 5% non-fat milk, and blotted with the indicated primary antibodies, followed by HRP-conjugated secondary antibodies. Loading of equal amount of protein was confirmed by blotting with anti-GAPDH antibody (HyTest Ltd., Turku, Finland). The various bands were visualized by enhanced chemiluminescence, using ECL reagent and ECL Hyperfilm (Amersham, Quebec, Canada). All experiments were conducted for at least three times, and all blots were analyzed using Scion Image software for Windows (Scion Corporation, Frederick, MD).

Immunofluorescence

Cells were plated on glass cover slips and were grown for 3 days, prior to treatment with copper or zinc in the absence or presence of 30 μM PD98059. Cells were fixed in ice-cold methanol for 10 min, washed twice with PBS, and fixed with 4% paraformaldehyde for additional 20 min. Prior to staining, cells were permeabilized with 0.2% Triton X-100 and blocked with 5% normal goat serum (NGS) in PBS. These cells were incubated overnight at 4°C with anti-p21 (1:200 dilution), anti-p53 (1:200), or anti-AIF (1:500) in PBS containing 1% NGS. Positive cells were visualized using goat anti-rabbit fluorescein isothocyanate (FITC) conjugated secondary antibody. Cells were visualized using a Zeiss Axiovert 100 TV fluorescence microscope (Carl Zeiss, Germany).

Data Analysis

Data are presented as means ± SE of three to five independent experiments. Densitometric quantitation of Western immunoblots was performed using Scion Image program. Statistical analysis was performed using two-group comparisons by means of Student's *t*-test; a *P*-value below 0.05 was considered statistically significant.

RESULTS

Metal-Induced Activation of ERK

In this study, we examined whether extracellular copper and zinc can activate the ERK in epithelial breast cancer cells with different p53 status, and investigate the relationship between changes in ERK phosphorylation and metal induced apoptosis. The time course of copper- and zinc-induced ERK phosphorylation in MDA-MB231, MCF7, and MCF7-E6 cells is illustrated in Figure 1. The levels of phosphorylated ERK, which represent ERK activities, were increased within 2 h in MDA-MB-231 cells, with mutated p53, exposed to copper at and zinc at all dosages studied. The strongest increase in ERK phosphorylation was observed in

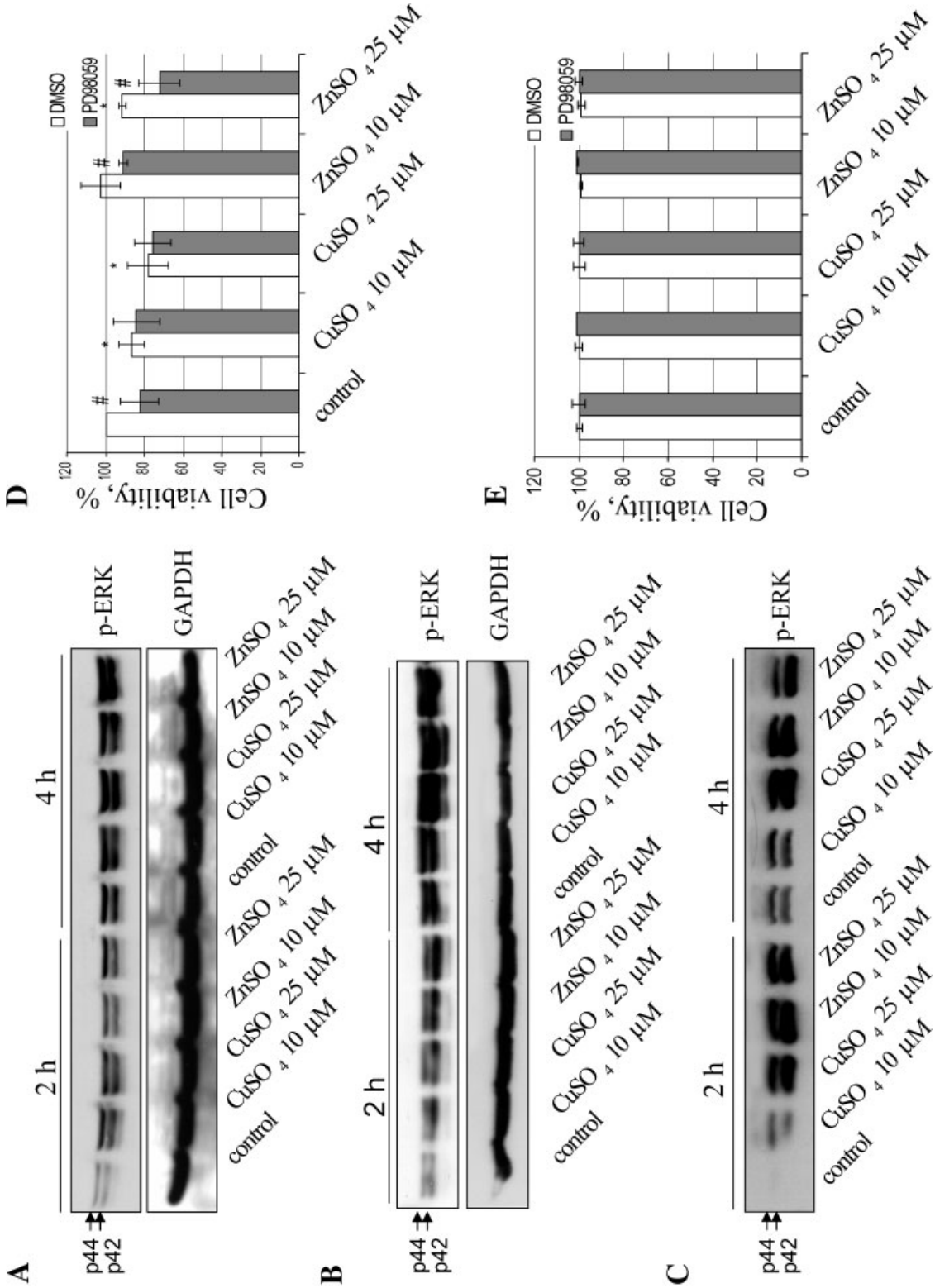
A
2 h
4 h
p-ERK
GAPDH
p44
p42
control
CuSO 4 10 μM
CuSO 4 25 μM
ZnSO 4 10 μM
ZnSO 4 25 μM
B
C
D
DMSO
PD98059
Cell viability, %
E

Fig. 1.

MDA-MB231 cells exposed to zinc at 10 and 25 μM. Activation of ERK was sustained for 4 h after copper and zinc treatments. There was only slight induction of ERK by either copper or zinc after 2 and 4 h exposure in MCF7 cells with wild p53. In contrast to effect of metals in MDA-MB231 cells, the strongest increase in ERK activity in MCF7 cells was observed after exposure to copper. Disruption of p53 wild-type function in MCF7 cells by transfection with human papilomavirus type E6 gene resulted in an increased phosphorylation of ERK in the presence of copper and zinc similar to that observed in MDA-MB-231 cells with mutated p53. Only MCF7 cells with functional p53 had shown a decrease in cell viability after treatment with either copper or zinc (Fig. 1D). Therefore, the strong and prolonged activation of ERK induced by metals in highly metastatic MDA-MB231 cells may relate to their resistance to metal induced stress, whereas weak ERK activation in response to metal treatment makes non-metastatic MCF7 cells vulnerable to the metal toxicity. Furthermore, the blockade of ERK by MEK inhibition through addition of PD98059 caused a decrease in cell viability in MCF7 cells, however, combined treatment with metals did not result in synergistic toxicity. MDA-MB231 cells, with mutated p53, were resistant to metals and PD98059. Increased cell death by MEK inhibitor was observed only in p53 positive MCF7 cells indicating that the suppression of MEK/ERK signaling pathway may stabilize p53 protein.

Effect of PD98059 on Metal-Induced Cell Death

There are several methods to evaluate apoptosis. Determination of a change in the mitochondrial membrane potential ($\Delta\Psi_m$), which results in mitochondrial membrane permeabilization, is one of the important characteristics of early apoptosis [Zamzami et al., 1996]. In order to examine whether cell death is related to ERK activation, we used MEK inhibitor PD98059 that prevents ERK phosphorylation. We used JC-1 staining to determine the change in mitochondrial membrane potential in three cell lines with different p53 status, pretreated with or without PD98059, and exposed to copper and zinc. The loss of mitochondrial membrane potential was found only in MCF7 cells after 4 h exposure to copper and zinc at 10 and 25 μM, whereas there was no such effect in MCF7-E6 (where p53 is inactivated) and MDA-MB-231 cells with mutated p53 (Fig. 2A). The treatment of the p53-mutated MDA-MB231 cells with MEK inhibitor revealed no difference in the $\Delta\Psi_m$, whereas PD98059 caused a strong decrease in the $\Delta\Psi_m$ exclusively in MCF7 cells. The incubation of MCF7 cells with PD98059 and followed by treatment with metals did not result in synergistic toxicity. However, the combined treatment resulted in the loss of mitochondrial membrane potential up to the same level as MEK inhibitor alone. These data were confirmed by using Hoechst 33342 staining (Fig. 2D). After 4 h of treatment, copper at 25 μM caused an increase in the number of apoptotic cells in MCF7 cells compared to control cells demonstrated by Hoechst 33342 staining. Zinc at 25 μM also resulted in increase in the number of apoptotic cells, although to lesser extent than copper. Pretreatment of MCF7 cells with PD98059 resulted in an increase in amount of apoptotic cells (Fig. 2D). However, exposure of MCF7 cells to either copper or zinc after pretreatment with PD98059 did not significantly change the number of apoptotic cells. Figures 2A,B shows comparative alterations in MCF7 cells after pretreatment with or without PD98059, and exposure to copper and zinc. Treatment of MCF7 cells with an inhibitor of p53 pifithrin-α at 15 μM concentration partly restored the decline in mitochondrial membrane potential, stimulated by copper and zinc (Fig. 2B). Moreover, blocking of p53 prevented PD98059 induced breakdown of the $\Delta\Psi_m$, supporting the important role of p53. Taken together, these findings demonstrate

Fig. 1. Phosphorylation of ERK1/2 in MCF7 (p53+/ER+) (**A**), MCF7-E6 (p53−/ER+) (**B**), and MDA-MB 231 (p53−/ER−) (**C**) cells after exposure to copper and zinc and the effect of ERK inhibition on cell viability in copper and zinc treated MCF7 (**D**) and MDA-MB 231 (**E**) cells. These cells were treated with copper at 10 and 25 μM or zinc at 10 and 25 μM in serum-free medium for 2 and 4 h. The ERK phosphorylation, which represents ERK activity, was determined using phosphor-specific antibodies. To determine the effect of ERK inhibition on the cell viability, the cells were pretreated with 30 μM of PD98059 for 1 h. Then the cells were exposed to 25 μM of copper or 25 μM of zinc for additional 4 h. MTT (3-(4,5-dimethylthiazol-2-yl)-2,5-diphenyl tetrazolium bromide) was used to test the cell viability. Results are presented as means ± SE of four independent experiments ($P < 0.05$). The asterisk sign (*) denotes values versus control (with DMSO), whereas the pound sign (#) stands for samples treated with PD98059 versus samples without inhibitor.

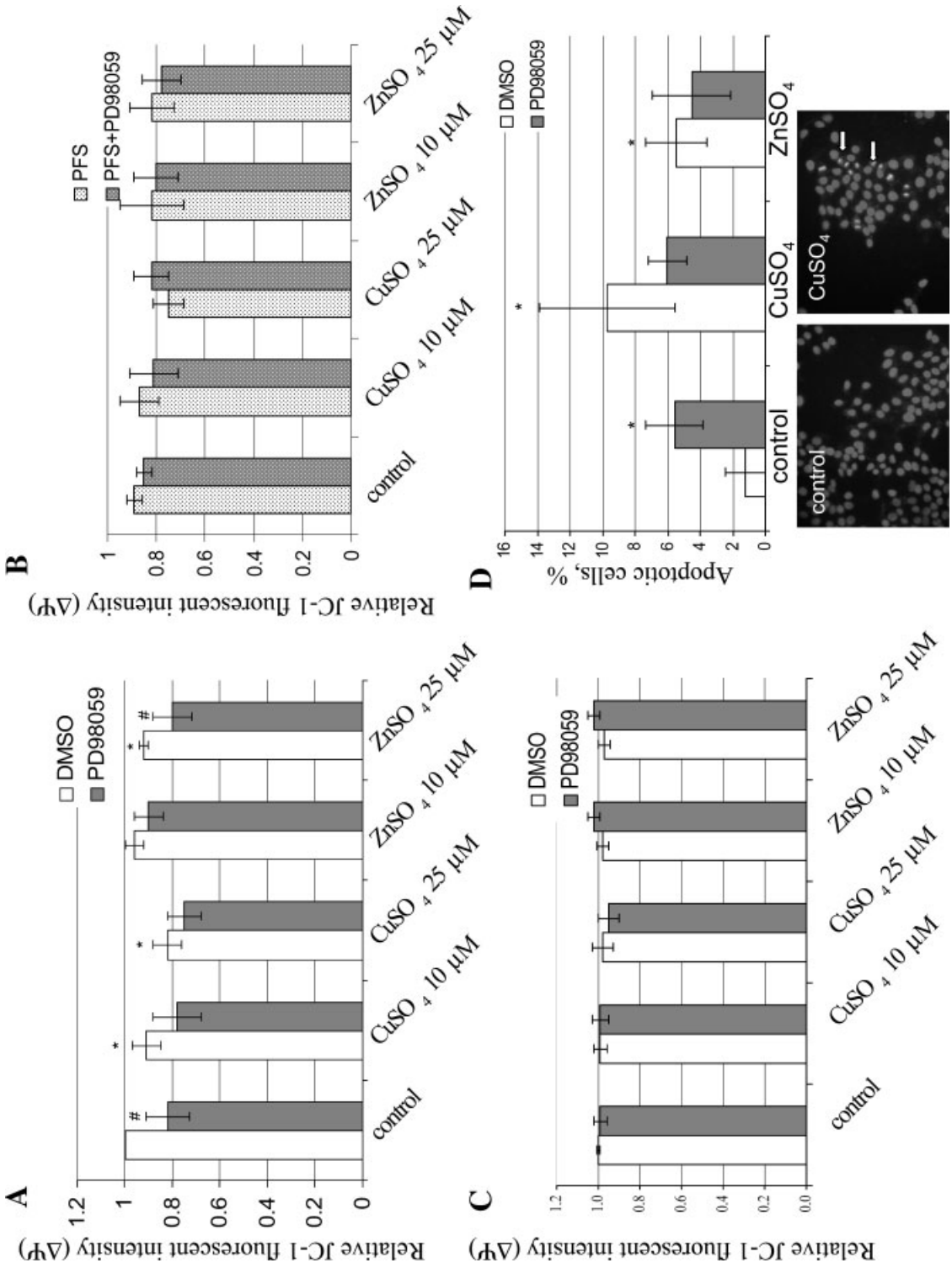
A
Relative JC-1 fluorescent intensity (ΔΨ)
DMSO
PD98059
control
CuSO 4 10 μM
CuSO 4 25 μM
ZnSO 4 10 μM
ZnSO 4 25 μM
B
Relative JC-1 fluorescent intensity (ΔΨ)
PFS
PFS+PD98059
C
Relative JC-1 fluorescent intensity (ΔΨ)
D
Apoptotic cells, %
CuSO4
ZnSO4

Fig. 2.

that suppression of MEK/ERK signaling pathway markedly induces apoptosis accompanied with dissipation of the mitochondrial inner membrane potential and this may be caused by p53 activation.

Activation of p53, $p21^{Waf17Cip1}$, and Bax by Metals Did Not Depend on Activation of ERK

To determine how PD98059 may cause apoptosis in MCF7 cells, the level of p53 and $p21^{CIP1/Waf1}$ proteins were analyzed by Western immunoblotting. A typical Western blot is shown in Figure 3A with densitometric scans of the blots for $p21^{CIP1/Waf1}$ from three separate experiments. PD98059 at 30 μM caused a complete inhibition of both the copper and zinc induced phosphorylation of ERK1/2. Inhibition of ERK in MCF7 cells through addition of PD98059 resulted in strong increase in expression of p53 accompanied by an increase in $p21^{CIP1/Waf1}$. However, p53 and p21 induction stimulated by copper and zinc remained unchanged when MCF7 cells were pretreated with PD98059. Therefore, copper and zinc induced increase of p53 and p21 was MEK/ERK independent. However, suppression of ERK signaling pathway by PD98059 triggers activation of p53 resulting in expression of pro-apoptotic p53 target gene products, such as p21 and Bax (Fig. 3A,B).

Induction of ROS Production by PD98059

In attempt to further characterize the effect of PD98059 in MCF7 cells, we measured generation of reactive oxygen species by using fluorescent probe DHR. Both copper and zinc exposures led to an increase in ROS generation in MCF7 cells (Fig. 4A), whereas the level of ROS production in MDA-MB-231 cells treated with copper and zinc remained unchanged (Fig. 4C). PD98059 alone stimulated generation of ROS only in MCF7 cells with wild-type p53 (Fig. 4A). We have results to indicate that effect of PD98059 was not due to fluorescence of the compound itself (data not shown). There was no enhancing effect of metals when pretreatment with MEK inhibitor was combined with metals, whereas the increase in ROS accumulation was stronger than in the presence of either copper or zinc alone. Suppression of MEK/ERK pathway resulted in steady increase in ROS production only in cells with wild-type p53, whereas disruption of p53 prevented effect of PD98059. Therefore, we conclude that suppression of MEK/ERK pathway in epithelial breast cancer MCF7 cells results in increase in ROS generation through activation of p53. The increase in ROS production in the presence of copper and zinc as well as in the presence of MEK inhibitor correlated with activation of $p21^{Cip1/WAF1}$ regulated by p53 in MCF7 cells (Fig. 4D).

Effect of PD98059 on Release of AIF

Immunostaining was used to examine the effect of PD98059 on AIF localization in MCF7 cells with and without metals. AIF translocation from mitochondria to the nucleus was initiated in response to PD98059 (Fig. 5). Exposure of MCF7 cells to copper stimulated release of AIF from mitochondria, but this effect was not further increased by pretreatment with PD98059. Zinc treatment did not stimulate the AIF relocation, whereas in the presence of MEK inhibitor it caused the release of AIF from mitochondria and was similar to that by the inhibitor alone. Thus, the effect of PD98059 provides evidence that suppression of MAPK kinase can result in apoptosis via disruption of mitochondrial membrane with the release of AIF.

DISCUSSION

MAP kinase is an important regulatory signal in breast cancer. Inhibitors of MAP kinase have been reported to block the growth of MCF7 cells, indicating a role for MEK/ERK pathway in cell

Fig. 2. Effect of PD98059 on $\Delta\Psi_m$ in MCF7 (**A, B**) and MDA-MB231 (**C**) cells as well as on apoptosis in MCF7 cells (**D**). The cells were incubated with 30 μM of PD98059 for 1 h with subsequent treatment with 25 μM of copper and 25 μM of zinc for additional 4 h. The changes in $\Delta\Psi_m$ were determined by staining with 10 μM of JC-1 for 10 min. In case (**B**), MCF7 cells were additionally incubated with 30 μM of pifithrin-α alone or combined with 30 μM of PD98059 for 1 h. Then the cells were exposed to 25 μM of copper or 25 μM of zinc for additional 4 h and $\Delta\Psi_m$ was determined. Results are from four independent experiments and are shown with error bars. **D**: The effects of copper and zinc in the absence or presence of PD98059 on apoptosis in MCF7 cells. The cells were incubated with 30 μM of PD98059 for 1 h followed by treatment with copper at 25 μM or zinc at 25 μM for additional 4 h. After staining with Hoechst 33342 apoptotic cells displayed condensed chromatin and fragmented nuclei (inserted images). Results are presented as means ± SE of five independent experiments ($P < 0.05$). The asterisk sign (*) denotes values versus control, whereas the pound sign (#) stands for samples treated with PD98059 versus samples without inhibitor.

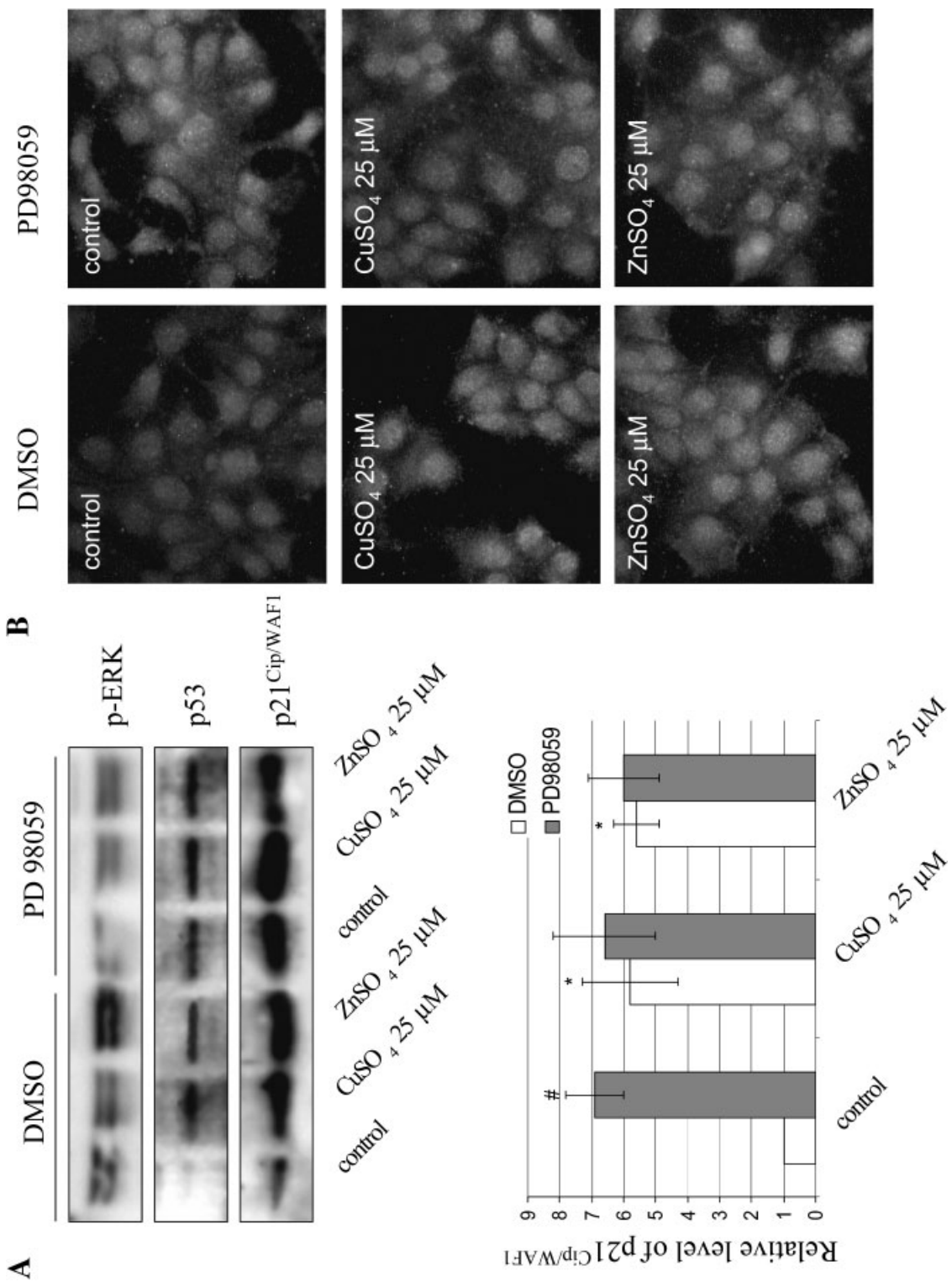
A
DMSO
PD 98059
p-ERK
p53
p21Cip/WAF1
control
ZnSO 4 25 µM
CuSO 4 25 µM
control
ZnSO 4 25 µM
CuSO 4 25 µM
B
DMSO
PD98059
control
CuSO4 25 µM
ZnSO4 25 µM
control
CuSO4 25 µM
ZnSO4 25 µM
DMSO
PD98059
Relative level of p21Cip/WAF1
0
1
2
3
4
5
6
7
8
9
#
*
*
control
CuSO 4 25 µM
ZnSO 4 25 µM

Fig. 3.

proliferation [Jeng et al., 2000]. Metal-induced activation of MAPK has been demonstrated in human bronchial epithelial cells [Samet et al., 1998]. In the present study, we have demonstrated a marked metal-induced activation of ERK in p53 mutated breast cancer MDA-MB-231 cells that lacked ER and G protein coupled receptor. Our data suggest that activation of ERK by metals in these cells most likely involves activation of Src as its kinase. Although both copper and zinc can activate ERK in ER positive non-metastatic MCF7 and MCF7-E6 cells, the disruption of p53 in MCF7-E6 cells resulted in a much higher magnitude of alteration in ERK phosphorylation induced by metals, similar to that found in highly metastatic MDA-MB-231 cells. Our results provide further evidence that regulation of ERK by metals in epithelial breast cancer cells depends not only on the ER status of cells but rather also on the p53 status. Our data are consistent with recent studies, which provided evidence for ERK downregulation by activated p53 [Nair et al., 2004]. Recently, it has been reported that MAP kinases can mediate regulation of p53 [Wu, 2004]. p53 can be regulated by Raf/MEK/ERK kinase pathway either via upregulation of $p19^{ARF}$ or induction of MDM2, a major negative regulator of p53 [Palmero et al., 1998; Tao and Levine, 1999; Ries et al., 2000; McMahon and Woods, 2001]. However, upregulation of $p19^{ARF}$ seems most unlikely since metal toxicity causes p53 activation through DNA damage, which does not depend on $p19^{ARF}$ [Kamijo et al., 1997]. Therefore, the activation of MEK/ERK kinase pathway can result in an increase in MDM2 protein levels with an increase in degradation of p53 [Ries et al., 2000]. Consistent with MEK/ERK pathway contribution to p53 dissipation, we present here that PD98059, MEK inhibitor, stimulated p53 accumulation and p53 function, as demonstrated by an increased level of p53-dependent $p21^{CIP1/Waf1}$, as well as Bax. Thus MAP kinases play a negative role in p53 regulation perhaps through upregulation of MDM2, transcriptional target of the Raf/MEK/ERK. Exposure of MCF7 cells to either copper or zinc resulted in strong increase in p53, and $p21^{CIP1/Waf1}$ protein levels, whereas inhibition of ERK activity did not affect the metal-induced p53 activation. These findings indicate that while MEK/ERK pathway is responsible for degradation of p53, this pathway is not involved in metal-induced activation of p53.

In consideration of the involvement of ROS as upstream regulators of p53 (as inducers of DNA damage) and downstream regulators of p53, and also the control of several genes regulated by p53 including PIGs on ROS generation, [Li et al., 1997a,b, 1999; Polyak et al., 1997], we studied the effect of ERK inhibition on ROS production in the presence of copper and zinc. Redox active copper is a well known and the most potent inducer of ROS generation and apoptosis [Pourahmad and O'Brien, 2000; Narayanan et al., 2001; Gyulkhandanyan et al., 2003; Ostrakhovitch and Cherian, 2004], while redox inactive zinc is considered as an inhibitor of apoptosis in various cell types [Barbieri et al., 1992]. However, recently there have been reports suggesting that, at certain concentrations, zinc can induce apoptosis through p53 overexpression and ROS generation that leads to apoptosis in various types of cells [Sensi et al., 1999; Gazaryan et al., 2002; Provinciali et al., 2002; Ryu et al., 2002; Ostrakhovitch and Cherian, 2004, 2005]. The present study demonstrates that zinc, similarly to copper, can induce activation of p53 protein and ROS generation in MCF7 cells, although such an increase in ROS production was not observed in p53 mutated MDA-MB-231 cells and p53 depleted MCF7-E6 cells when exposed to metals. Moreover, the generation of ROS could also affect ERK acti-

Fig. 3. Effect of ERK inhibition on p53, p21 expression (**A**), and Bax staining (**B**) in p53 positive MCF7 cells exposed to copper and zinc. MCF7 cells were incubated with 30 μM of PD98059 for 1 h and then treated with 25 μM of copper or 25 μM of zinc for additional 4 h in serum-free medium. Expression of p53, p21 proteins was determined by Western immunoblotting analysis. Bax expression was assessed by immunostaining with anti-Bax antibodies. PD98059 inhibited ERK phoshorylation mediated by copper and zinc thus confirming the specificity of the effects of MEK inhibitor. It also dramatically increased the levels of p53, p21, and Bax. The values shown are the means of three independent experiments ($P < 0.05$). The asterisk sign (*) denotes values versus control (with DMSO).

Fig. 4. (*Overleaf*) Effect of PD98059 on DCF fluorescence in p53-positive and negative cell lines exposed to copper and zinc. MCF7 (**A**), MCF7-E6 (**B**), and MDA-MB231 (**C**) cells pretreated with 20 μM of DCFH-DA for 30 min prior to addition of 30 μM of PD98059. Copper and zinc were added in 1 h for additional for 4 h. **D**: Correlation between ROS production and expression of $p21^{Cip/WAF1}$. Expression of $p21^{Cip/WAF1}$ was plotted versus relative increase in DCF fluorescence. The values shown are the means of four independent experiments ($P < 0.05$). The asterisk sign (*) denotes values versus control (with DMSO).

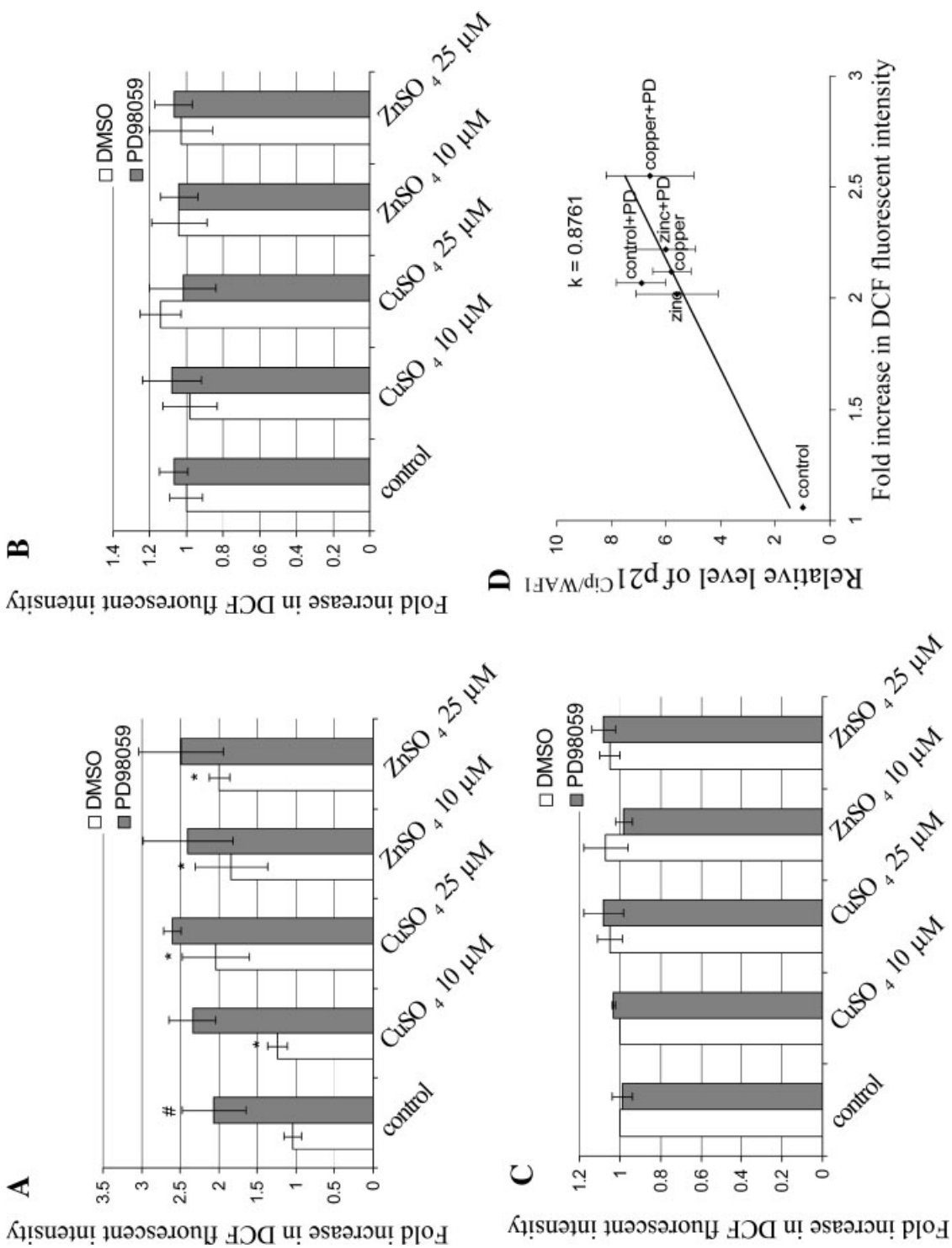
A
Fold increase in DCF fluorescent intensity
DMSO
PD98059
control
CuSO4 10 μM
CuSO4 25 μM
ZnSO4 10 μM
ZnSO4 25 μM
B
Fold increase in DCF fluorescent intensity
DMSO
PD98059
control
CuSO4 10 μM
CuSO4 25 μM
ZnSO4 10 μM
ZnSO4 25 μM
C
Fold increase in DCF fluorescent intensity
DMSO
PD98059
control
CuSO4 10 μM
CuSO4 25 μM
ZnSO4 10 μM
ZnSO4 25 μM
D
Relative level of p21Cip/WAF1
Fold increase in DCF fluorescent intensity
k = 0.8761
control
zinc
copper
control+PD
zinc+PD
copper+PD

Fig. 4.

Fig. 5. Inhibition of ERK causes the release of AIF in MCF7 cells. Redistribution of AIF in MCF 7 cells was assessed by immunofluorescent staining with anti-AIF antibodies. MCF7 cells were incubated with 30 µM of PD98059 for 1 h and then exposed to 25 µM of copper or 25 µM of zinc for additional 4 h in serum-free medium. Then, percent of cells with nuclear localized AIF was determined. The values shown are means of four independent experiments. The asterisk sign (*) denotes values versus control ($P < 0.05$).

vation in response to metals since it is known that ROS activate ERK [Guyton et al., 1996]. However, the lowest level of ERK phosphorylation corresponded to accumulation of ROS in MCF7 cells, exposed to metals, whereas the strongest increase in phosphorylation of ERK in response to copper and zinc exposure was observed in MDA-MB-231 cells in which metals were unable to increase the ROS production. These findings suggest that metal-induced ERK activation does not depend on ROS accumulation mediated by metals. However, there is a strong correlation between metal-induced ROS generation and expression of $p21^{CIP1/Waf1}$, the downstream target of p53. Pre-exposure to PD98059 without metal treatment dramatically increased the formation of ROS in MCF7 but did not affect the ROS levels in MCF7-E6 and MDA-MB231 cells. Pretreatment with PD98059 also increased metal induced ROS production. Since PD98059 increased the ROS production only in MCF7 cells with functional p53, the activation of p53 might be the main trigger in the stimulation of ROS generation. Thus the actual mechanism may be the blockage of MEK/ERK pathway resulting in activation of p53 that itself can cause generation of ROS. Consistent with our findings, the ability of PD98059 to trigger the ROS formation has been reported in PC12 pheochromocytoma cells expressing wild-type p53 [Cerioni et al., 2003].

The p53-mediated expression and direct translocation of Bax protein to the mitochondria, as well as ROS generation trigger opening of permeability transition pores that result in permeabilization of the outer mitochondria membrane [Schuler et al., 2000; Skulachev, 2002; Chipuk et al., 2003, 2004]. We demonstrate here that the complete blockage of ERK activation by MEK inhibition can cause disruption of the mitochondrial membrane integrity associated with apoptosis in MCF7 cells expressing wild p53. Additional evidence for the involvement of p53 in PD98059 induced mitochondrial breakdown is from the data showing that inhibition of p53 by pifithrin-α partially prevented the dissipation of mitochondrial membrane potential. The attenuation of $\Delta\Psi$ is mediated by opening of permeability transition pore thereby releasing proapoptotic proteins such as cytochrome-*c* and AIF from the intermembrane space [Martinou et al., 2000]. Since MCF7 cells are depleted in caspase 3, AIF seems to be the more likely executor of apoptosis in these cells [Janicke et al., 1998]. In our study, only copper but not zinc caused AIF redistribution from mitochondria to the nucleus, while both metals equally increased p53 and Bax protein levels. The weak ERK activation in MCF7 cells induced by copper was linked to cell death via nuclear relocation of AIF. The most notable aspect of our research was that suppression of ERK activity by treatment with PD98059 induced nuclear localization of AIF in MCF7 cells. However, inactivation of ERK did not increase sensitization of MCF7 cells toward metal toxicity.

In summary, our results indicate that MEK/ERK pathway mediates anti apoptotic signaling events in human breast cancer cells, but it may not play a role in metal-induced toxicity and cell death. However, suppression of ERK leads to activation of p53 and its downstream targets resulting in ROS production, dissipation of mitochondrial membrane integrity, and finally the cell death via nuclear relocation of AIF. Thus p53 may play a significant role in activation of ROS and apoptosis in cells deficient in caspases, such as breast cancer MCF7 cells.

REFERENCES

Arnoult D, Parone P, Martinou JC, Antonsson B, Estaquier J, Ameisen JC. 2002. Mitochondrial release of apoptosis-inducing factor occurs downstream of cytochrome c release in response to several proapoptotic stimuli. J Cell Biol 159:923–929.

Barbieri D, Troiano L, Grassilli E, Agnesini C, Cristofalo EA, Monti D, Capri M, Cossarizza A, Franceschi C. 1992. Inhibition of apoptosis by zinc: A reappraisal. Biochem Biophys Res Commun 187:1256–1261.

Cavallo F, Gerber M, Marubini E, Richardson S, Barbieri A, Costa A, DeCarli A, Pujol H. 1991. Zinc and copper in breast cancer. A joint study in northern Italy and southern France. Cancer 67:738–745.

Cerioni L, Palomba L, Cantoni O. 2003. The Raf/MEK inhibitor PD98059 enhances ERK1/2 phosphorylation mediated by peroxynitrite via enforced mitochondrial formation of reactive oxygen species. FEBS Lett 547:92–96.

Chipuk JE, Maurer U, Green DR, Schuler M. 2003. Pharmacologic activation of p53 elicits Bax-dependent apoptosis in the absence of transcription. Cancer Cell 4:371–381.

Chipuk JE, Kuwana T, Bouchier-Hayes L, Droin NM, Newmeyer DD, Schuler M, Green DR. 2004. Direct activation of Bax by p53 mediates mitochondrial membrane permeabilization and apoptosis. Science 303: 1010–1014.

Cregan SP, Fortin A, MacLaurin JG, Callaghan SM, Cecconi F, Yu SW, Dawson TM, Dawson VL, Park DS, Kroemer G, Slack RS. 2002. Apoptosis-inducing factor is involved in the regulation of caspase-independent neuronal cell death. J Cell Biol 158:507–517.

Cross TG, Scheel-Toellner D, Henriquez NV, Deacon E, Salmon M, Lord JM. 2000. Serine/threonine protein kinases and apoptosis. Exp Cell Res 256:34–41.

Daugas E, Susin SA, Zamzami N, Ferri KF, Irinopoulou T, Larochette N, Prevost MC, Leber B, Andrews D, Penninger J, Kroemer G. 2000. Mitochondrio-nuclear translocation of AIF in apoptosis and necrosis. FASEB J 14:729–739.

Degli EM, Dive C. 2003. Mitochondrial membrane permeabilisation by Bax/Bak. Biochem Biophys Res Commun 304:455–461.

Drake EN, Sky-Peck HH. 1989. Discriminant analysis of trace element distribution in normal and malignant human tissues. Cancer Res 49:4210–4215.

Feng P, Liang JY, Li TL, Guan ZX, Zou J, Franklin R, Costello LC. 2000. Zinc induces mitochondria apoptogenesis in prostate cells. Mol Urol 4:31–36.

Feng P, Li TL, Guan ZX, Franklin RB, Costello LC. 2002. Direct effect of zinc on mitochondrial apoptogenesis in prostate cells. Prostate 52:311–318.

Feng P, Li TL, Guan ZX, Franklin RB, Costello LC. 2003. Effect of zinc on prostatic tumorigenicity in nude mice. Ann NY Acad Sci 1010:316–320.

Fonfria E, Dare E, Benelli M, Sunol C, Ceccatelli S. 2002. Translocation of apoptosis-inducing factor in cerebellar granule cells exposed to neurotoxic agents inducing oxidative stress. Eur J Neurosci 16:2013–2016.

Gazaryan IG, Krasnikov BF, Ashby GA, Thorneley RN, Kristal BS, Brown AM. 2002. Zinc is a potent inhibitor of thiol oxidoreductase activity and stimulates reactive oxygen species production by lipoamide dehydrogenase. J Biol Chem 277:10064–10072.

Guyton KZ, Liu Y, Gorospe M, Xu Q, Holbrook NJ. 1996. Activation of mitogen-activated protein kinase by H2O2. Role in cell survival following oxidant injury. J Biol Chem 271:4138–4142.

Gyulkhandanyan AV, Feeney CJ, Pennefather PS. 2003. Modulation of mitochondrial membrane potential and reactive oxygen species production by copper in astrocytes. J Neurochem 87:448–460.

Halaschek-Wiener J, Wacheck V, Kloog Y, Jansen B. 2004. Ras inhibition leads to transcriptional activation of p53 and down-regulation of Mdm2: Two mechanisms that cooperatively increase p53 function in colon cancer cells. Cell Signal 16:1319–1327.

Hansson A. 1996. Extracellular zinc ions induces mitogen-activated protein kinase activity and protein tyrosine phosphorylation in bombesin-sensitive Swiss 3T3 fibroblasts. Arch Biochem Biophys 328:233–238.

Huang YL, Sheu JY, Lin TH. 1999. Association between oxidative stress and changes of trace elements in patients with breast cancer. Clin Biochem 32:131–136.

Janicke RU, Sprengart ML, Wati MR, Porter AG. 1998. Caspase-3 is required for DNA fragmentation and morphological changes associated with apoptosis. J Biol Chem 273:9357–9360.

Jeng MH, Yue W, Eischeid A, Wang JP, Santen RJ. 2000. Role of MAP kinase in the enhanced cell proliferation of long term estrogen deprived human breast cancer cells. Breast Cancer Res Treat 62:167–175.

Jin R, Bay B, Tan P, Tan BK. 1999. Metallothionein expression and zinc levels in invasive ductal breast carcinoma. Oncol Rep 6:871–875.

Kamijo T, Zindy F, Roussel MF, Quelle DE, Downing JR, Ashmun RA, Grosveld G, Sherr CJ. 1997. Tumor suppression at the mouse INK4a locus mediated by the alternative reading frame product p19ARF. Cell 91:649–659.

Koksoy C, Kavas GO, Akcil E, Kocaturk PA, Kara S, Ozarslan C. 1997. Trace elements and superoxide dismutase in benign and malignant breast diseases. Breast Cancer Res Treat 45:1–6.

Kondoh M, Tasaki E, Araragi S, Takiguchi M, Higashimoto M, Watanabe Y, Sato M. 2002. Requirement of caspase and p38MAPK activation in zinc-induced apoptosis in human leukemia HL-60 cells. Eur J Biochem 269:6204–6211.

Kuo HW, Chen SF, Wu CC, Chen DR, Lee JH. 2002. Serum and tissue trace elements in patients with breast cancer in Taiwan. Biol Trace Elem Res 89:1–11.

Li PF, Dietz R, von Harsdorf R. 1997a. Differential effect of hydrogen peroxide and superoxide anion on apoptosis and proliferation of vascular smooth muscle cells. Circulation 96:3602–3609.

Li PF, Dietz R, von Harsdorf R. 1997b. Reactive oxygen species induce apoptosis of vascular smooth muscle cell. FEBS Lett 404:249–252.

Li PF, Dietz R, von Harsdorf R. 1999. p53 regulates mitochondrial membrane potential through reactive oxygen species and induces cytochrome c-independent apoptosis blocked by Bcl-2. EMBO J 18:6027–6036.

Liang JY, Liu YY, Zou J, Franklin RB, Costello LC, Feng P. 1999. Inhibitory effect of zinc on human prostatic carcinoma cell growth. Prostate 40:200–207.

Makin G, Dive C. 2001. Modulating sensitivity to drug-induced apoptosis: The future for chemotherapy? Breast Cancer Res 3:150–153.

Martinou JC, Desagher S, Antonsson B. 2000. Cytochrome c release from mitochondria: All or nothing. Nat Cell Biol 2:E41–E43.

Marzo I, Brenner C, Zamzami N, Jurgensmeier JM, Susin SA, Vieira HL, Prevost MC, Xie Z, Matsuyama S, Reed JC, Kroemer G. 1998. Bax and adenine nucleotide translocator cooperate in the mitochondrial control of apoptosis. Science 281:2027–2031.

McMahon M, Woods D. 2001. Regulation of the p53 pathway by Ras, the plot thickens. Biochim Biophys Acta 1471:M63–M71.

Miyashita T, Reed JC. 1995. Tumor suppressor p53 is a direct transcriptional activator of the human bax gene. Cell 80:293–299.

Miyashita T, Harigai M, Hanada M, Reed JC. 1994a. Identification of a p53-dependent negative response element in the bcl-2 gene. Cancer Res 54:3131–3135.

Miyashita T, Krajewski S, Krajewska M, Wang HG, Lin HK, Liebermann DA, Hoffman B, Reed JC. 1994b. Tumor suppressor p53 is a regulator of bcl-2 and bax gene expression in vitro and in vivo. Oncogene 9:1799–1805.

Myhre O, Andersen JM, Aarnes H, Fonnum F. 2003. Evaluation of the probes 2′,7′-dichlorofluorescin diacetate, luminol, and lucigenin as indicators of reactive species formation. Biochem Pharmacol 65:1575–1582.

Nair VD, Yuen T, Olanow CW, Sealfon SC. 2004. Early single cell bifurcation of pro- and antiapoptotic states during oxidative stress. J Biol Chem 279:27494–27501.

Nakano K, Vousden KH. 2001. PUMA, a novel proapoptotic gene, is induced by p53. Mol Cell 7:683–694.

Narayanan VS, Fitch CA, Levenson CW. 2001. Tumor suppressor protein p53 mRNA and subcellular localization are altered by changes in cellular copper in human Hep G2 cells. J Nutr 131:1427–1432.

Narita M, Shimizu S, Ito T, Chittenden T, Lutz RJ, Matsuda H, Tsujimoto Y. 1998. Bax interacts with the permeability transition pore to induce permeability transition and cytochrome c release in isolated mitochondria. Proc Natl Acad Sci USA 95:14681–14686.

Oda E, Ohki R, Murasawa H, Nemoto J, Shibue T, Yamashita T, Tokino T, Taniguchi T, Tanaka N. 2000. Noxa, a BH3-only member of the Bcl-2 family and candidate mediator of p53-induced apoptosis. Science 288:1053–1058.

Ostrakhovitch EA, Cherian MG. 2004. Differential regulation of signal transduction pathways in wild type and mutated p53 breast cancer epithelial cells by copper and zinc. Arch Biochem Biophys 423:351–361.

Ostrakhovitch EA, Cherian MG. 2005. Role of p53 and reactive oxygen species in apoptotic response to copper and zinc in epithelial breast cancer cells. Apoptosis 10: 111–122.

Palmero I, Pantoja C, Serrano M. 1998. p19ARF links the tumour suppressor p53 to Ras. Nature 395:125–126.

Park KS, Ahn Y, Kim JA, Yun MS, Seong BL, Choi KY. 2002. Extracellular zinc stimulates ERK-dependent activation of p21(Cip/WAF1) and inhibits proliferation of colorectal cancer cells. Br J Pharmacol 137:597–607.

Pearson G, Robinson F, Beers GT, Xu BE, Karandikar M, Berman K, Cobb MH. 2001. Mitogen-activated protein (MAP) kinase pathways: Regulation and physiological functions. Endocr Rev 22:153–183.

Polyak K, Xia Y, Zweier JL, Kinzler KW, Vogelstein B. 1997. A model for p53-induced apoptosis. Nature 389: 300–305.

Pourahmad J, O'Brien PJ. 2000. A comparison of hepatocyte cytotoxic mechanisms for Cu2+ and Cd2+. Toxicology 143:263–273.

Provinciali M, Donnini A, Argentati K, Di Stasio G, Bartozzi B, Bernardini G. 2002. Reactive oxygen species modulate Zn(2+)-induced apoptosis in cancer cells. Free Radic Biol Med 32:431–445.

Ries S, Biederer C, Woods D, Shifman O, Shirasawa S, Sasazuki T, McMahon M, Oren M, McCormick F. 2000. Opposing effects of Ras on p53: Transcriptional activation of mdm2 and induction of p19ARF. Cell 103:321–330.

Ryu R, Shin Y, Choi JW, Min W, Ryu H, Choi CR, Ko H. 2002. Depletion of intracellular glutathione mediates zinc-induced cell death in rat primary astrocytes. Exp Brain Res 143:257–263.

Samet JM, Graves LM, Quay J, Dailey LA, Devlin RB, Ghio AJ, Wu W, Bromberg PA, Reed W. 1998. Activation of MAPKs in human bronchial epithelial cells exposed to metals. Am J Physiol 275:L551–L558.

Schuler M, Bossy-Wetzel E, Goldstein JC, Fitzgerald P, Green DR. 2000. p53 induces apoptosis by caspase activation through mitochondrial cytochrome c release. J Biol Chem 275:7337–7342.

Sebolt-Leopold JS, Herrera R. 2004. Targeting the mitogen-activated protein kinase cascade to treat cancer. Nat Rev Cancer 4:937–947.

Sensi SL, Yin HZ, Carriedo SG, Rao SS, Weiss JH. 1999. Preferential Zn2+ influx through Ca2+-permeable AMPA/kainate channels triggers prolonged mitochondrial superoxide production. Proc Natl Acad Sci USA 96:2414–2419.

Sewing A, Wiseman B, Lloyd AC, Land H. 1997. High-intensity Raf signal causes cell cycle arrest mediated by p21Cip1. Mol Cell Biol 17:5588–5597.

Shimizu S, Narita M, Tsujimoto Y. 1999. Bcl-2 family proteins regulate the release of apoptogenic cytochrome c by the mitochondrial channel VDAC. Nature 399:483–487.

Skulachev VP. 2002. Programmed death phenomena: from organelle to organism. Ann NY Acad Sci 959:214–237.

Stewart ZA, Pietenpol JA. 2001. p53 Signaling and cell cycle checkpoints. Chem Res Toxicol 14:243–263.

Susin SA, Lorenzo HK, Zamzami N, Marzo I, Snow BE, Brothers GM, Mangion J, Jacotot E, Costantini P, Loeffler M, Larochette N, Goodlett DR, Aebersold R, Siderovski DP, Penninger JM, Kroemer G. 1999. Molecular characterization of mitochondrial apoptosis-inducing factor. Nature 397:441–446.

Susin SA, Daugas E, Ravagnan L, Samejima K, Zamzami N, Loeffler M, Costantini P, Ferri KF, Irinopoulou T, Prevost MC, Brothers G, Mak TW, Penninger J, Earnshaw WC, Kroemer G. 2000. Two distinct pathways leading to nuclear apoptosis. J Exp Med 192:571–580.

Tao W, Levine AJ. 1999. P19(ARF) stabilizes p53 by blocking nucleo-cytoplasmic shuttling of Mdm2. Proc Natl Acad Sci USA 96:6937–6941.

Woods D, Parry D, Cherwinski H, Bosch E, Lees E, McMahon M. 1997. Raf-induced proliferation or cell cycle arrest is determined by the level of Raf activity with arrest mediated by p21Cip1. Mol Cell Biol 17:5598–5611.

Wu GS. 2004. The functional interactions between the p53 and MAPK signaling pathways. Cancer Biol Ther 3:156–161.

Xia Z, Dickens M, Raingeaud J, Davis RJ, Greenberg ME. 1995. Opposing effects of ERK and JNK-p38 MAP kinases on apoptosis. Science 270:1326–1331.

Yu J, Zhang L, Hwang PM, Kinzler KW, Vogelstein B. 2001. PUMA induces the rapid apoptosis of colorectal cancer cells. Mol Cell 7:673–682.

Zamzami N, Susin SA, Marchetti P, Hirsch T, Gomez-Monterrey I, Castedo M, Kroemer G. 1996. Mitochondrial control of nuclear apoptosis. J Exp Med 183:1533–1544.